Significant Differences in the Electrochemical Behavior of the α-, β-, γ-, and δ-Tocopherols (Vitamin E)

Gregory J. Wilson, Ching Yeh Lin, and Richard D. Webster*

Research School of Chemistry, Australian National University, Canberra ACT 0200, Australia

Received: January 23, 2006; In Final Form: April 16, 2006

α-, β-, γ-, and δ-Tocopherols can be oxidized in dry CH_2Cl_2 or CH_3CN by one electron to form cation radicals that deprotonate to form the neutral phenoxyl radicals, which are then immediately further oxidized by one electron to the phenoxonium cations (an ECE electrochemical mechanism, where E signifies an electron transfer and C represents a chemical step, with the electrochemical mechanism having been determined by in situ spectroscopic analysis). The principal difference in the electrochemical behavior of the tocopherols relates to the stability of their associated phenoxonium cations. The phenoxonium cation of α-tocopherol is stable in solution for at least several hours, the phenoxonium cation of β-tocopherol is stable for several minutes, and the phenoxonium cations of γ- and δ-tocopherol are stable for <1 s. In dry CH_2Cl_2 containing >0.75 M acid (CF_3COOH), the deprotonation reaction of the cation radicals can be completely inhibited resulting in the cyclic voltammetric behavior of the tocopherols appearing as chemically reversible one-electron oxidation processes (an E mechanism). In dry acid conditions, the cation radicals can be further oxidized by one electron to form the dications, which are unstable and immediately deprotonate. The high stability of the phenoxonium cation of α-tocopherol compared to the other tocopherols (and most other phenols) is a chemically important feature that may shed new light on understanding α-tocopherol's unique biological properties.

1. Introduction

Vitamin E refers to a collection of naturally occurring compounds produced by plants that are based on 6-chromanol with an extended alkyl (phytyl) chain in the 2-position, which gives the compounds oil-like properties. Vitamin E compounds with a saturated phytyl chain are designated tocopherols while tocotrienols are differentiated by the presence of double bonds in the 3′, 7′, and 11′ positions of the alkyl side chain (Chart 1). The α-, β-, γ-, and δ-forms of the tocopherols and tocotrienols can be further differentiated by the degree of methylation of the aromatic ring. It will be demonstrated in this work that the stability of the oxidized forms of the tocopherols differ markedly despite the close structural similarities that exist between the α-, β-, γ-, and δ-forms, and it is proposed that these differences may account for their specific non-antioxidant biological functions.

α-Tocopherol (α-TOH), the fully methylated tocopherol, is by far the most biologically active and abundant of all the components of vitamin E found in mammalian tissues. Extensive electrochemical experiments on α-TOH have proven the existence of several intermediate oxidized forms that are accessible in dry aprotic organic solvents such as CH_3CN and CH_2Cl_2 and are linked through proton and electron transfers (Scheme 1).[1−3] In acetonitrile at approximately neutral pH, α-TOH can be electrochemically oxidized by one electron at solid electrodes to form the cation radical (α-$TOH^{+\bullet}$). α-$TOH^{+\bullet}$ quickly dissociates into α-$TO^{\bullet}$ (and H^+), which is immediately further oxidized at the electrode surface by one electron to form the bright orange-red phenoxonium cation (α-TO^+; an ECE mechanism; Scheme 1, pathway 2).[1−3] α-TO^+ is stable for at least several hours in the absence of water and can be reduced back to α-TOH on both the cyclic voltammetry (seconds) and controlled potential electrolysis (hours) time scales.[2,3] α-TO^+ can also be formed by homogeneous chemical oxidation of α-TOH with 2 equiv of NO^+ in CH_3CN and can be generated in sufficient quantity to enable characterization by ^{13}C NMR spectroscopy.[3]

CHART 1: Structures of Vitamin E

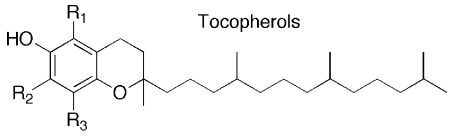

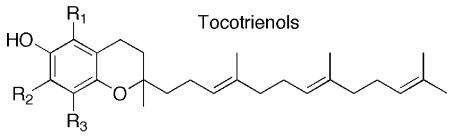

Tocopherol/ Tocotrienol	R_1	R_2	R_3
α-	CH_3	CH_3	CH_3
β-	CH_3	H	CH_3
γ-	H	CH_3	CH_3
δ-	H	H	CH_3

The addition of an equimolar amount of organo-soluble base (such as Et_4NOH) to CH_3CN solutions of α-TOH immediately forms the phenolate anion (α-TO^-),[4,5] which can be oxidized in two sequential one-electron steps to also form α-TO^+ (Scheme 1, pathway 3).[2] In the presence of ≳1−2% CF_3SO_3H, α-TOH is oxidized in two one-electron steps to form first α-$TOH^{+\bullet}$, and then at more positive potentials the dication (α-TOH^{2+}) is thought to be formed (Scheme 1, pathway 1).[1,2] It

* Author to whom correspondence should be addressed. Fax: + 61 2 6125 0750. E-mail: webster@rsc.anu.edu.au.

10.1021/jp0604802 CCC: $33.50
Published on Web 05/19/2006

SCHEME 1: Electrochemically Induced Transformations of α-TOH in Dry CH_3CN or CH_2Cl_2[2,3] [a]

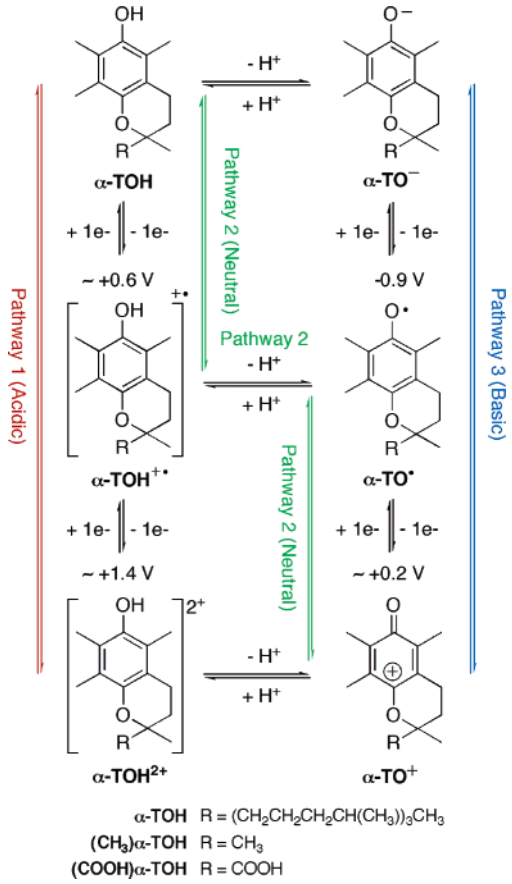

[a] One resonance structure is displayed for each compound. The listed potentials (vs Fc/Fc^+) were obtained by voltammetry and are the approximate values necessary to bring about oxidation of the phenolic compounds but do not necessarily correspond to the formal potential. The counterions for the charged species are the supporting electrolyte cation [Bu_4N^+] and anion [PF_6^-].

was found that substituting the R-group in Scheme 1 by a methyl group ((CH3)α-TOH)[1,3] or a carboxylic acid group ((COOH)α-TOH),[3] to form the simpler α-TOH model compounds, resulted in no change to the electrochemical behavior; thus the electrochemical responses shown in Scheme 1 are independent of the phytyl chain (and therefore not influenced by chirality effects).

This study is focused on comparing the electrochemical behavior of all of the tocopherols (α, β, γ, and δ) to determine whether they undergo the same mechanism as α-TOH (Scheme 1). We were also interested in establishing whether the dication of any of the tocopherols was sufficiently stable to enable spectroscopic characterization, by using very strong acid conditions to inhibit the potential deprotonation reaction.

2. Experimental Methods

2.1. Reagents. (±)-α-TOH (97%), (*R*)-(+)-6-hydroxy-2,5,7,8-tetramethylchroman-2-carboxylic acid (98%), and CF_3COOH (99+%) were obtained from Aldrich and stored in the dark under nitrogen. (±)-β-TOH (in hexane) (98%) was obtained from Supelco, and (+)-γ-TOH (96%) and (+)-δ-TOH (90%) were obtained from Sigma and stored in the dark at 277 K under nitrogen. 6-Hydroxy-2,2,5,7,8-pentamethylchroman was prepared by a published method.[6] Bu_4NPF_6 was prepared and purified by standard methods,[7] dried under vacuum at 413 K for 72 h, and stored under nitrogen. HPLC grade CH_2Cl_2 (EM Science) and CH_3CN (Labscan) were dried over calcium hydride (under nitrogen) and distilled immediately prior to use.

2.2. Apparatus. Cyclic voltammetric (CV) experiments were conducted with a computer-controlled Eco Chemie μAutolab III potentiostat using a planar 1 mm diameter Pt working electrode in conjunction with a Pt auxiliary electrode and an Ag wire reference electrode connected to the test solution via a salt bridge containing 0.5 M Bu_4NPF_6 in CH_3CN. Accurate potentials were obtained using ferrocene (Fc/Fc^+) as an internal standard.

Bulk electrolyzed solutions of the tocopherols (and model compounds) were prepared in a divided controlled potential electrolysis (CPE) cell separated with a porosity no. 5 (1.0−1.7 μm) sintered glass frit. The working and auxiliary electrodes were identically sized Pt mesh plates symmetrically arranged with respect to each other with an Ag wire reference electrode (isolated by a salt bridge) positioned to within 2 mm of the surface of the working electrode. The electrolysis cell was jacketed in a glass sleeve and cooled to 253 K using a Lauda RL6 variable temperature methanol-circulating bath. The volumes of both the working and the auxiliary electrode compartments were approximately 10 mL each. The solution in the working electrode compartment was simultaneously deoxygenated and stirred using bubbles of argon gas. The number of electrons transferred during the bulk oxidation process was calculated from

$$N = Q/n\mathrm{F} \qquad (1)$$

where N is the number of moles of the starting compound, Q is the charge (coulombs), n is the number of electrons, and F is the Faraday constant (96 485 C mol^{-1}).

In situ UV−vis spectra were obtained with a Varian Cary 5E spectrophotometer in an optically transparent thin layer electrochemical (OTTLE) cell (path length = 0.05 cm) using a Pt mesh working electrode.[2,8] The typical exhaustive electrolysis time for the one-electron oxidation of 1 mM analyte in CH_2Cl_2 (0.5 M Bu_4NPF_6) at 253 K was 1 h. In situ electrochemical Fourier transform infrared (FTIR) experiments were conducted with a Mettler Toledo ReactIR 4000 spectrometer utilizing a diamond composite attenuated total reflection (ATR) probe,[2,3,9] and electron paramagnetic resonance (EPR) experiments were performed on a Bruker ER200D spectrometer with a TE_{102} cavity.

2.3. Theoretical Calculations. Molecular orbital calculations were performed using a development version of the Q-Chem 2.1 software package[10] and the Spartan '04 software package.[11] Harmonic vibrational frequencies were calculated by Q-Chem using the EDF2/6-31+G* density functional model[12] and the SG-1 quadrature grid,[13] and no empirical scale factors were applied.

3. Results

3.1. Electrochemistry and UV−Vis Spectroscopy in CH_3CN. Cyclic voltammograms of 2 mM solutions of α-, β-, γ-, and δ-TOH in CH_3CN over a range of temperatures are shown in Figure 1. All the compounds displayed an oxidation peak (E_p^{ox}) at approximately +0.5 to +0.6 V vs Fc/Fc^+ with similar anodic peak current (i_p^{ox}) values indicating the transfer of the same number of electrons (i.e., $n = 2$).[2] The CV responses observed for α-TOH in neutral CH_3CN represent the pathway 2 series of reactions in Scheme 1, with the changing voltammetric shapes observed with varying temperature due to the rate and equilibrium constants for the proton-transfer reaction in Scheme 1 (eq 2) shifting with changing conditions and due to specific

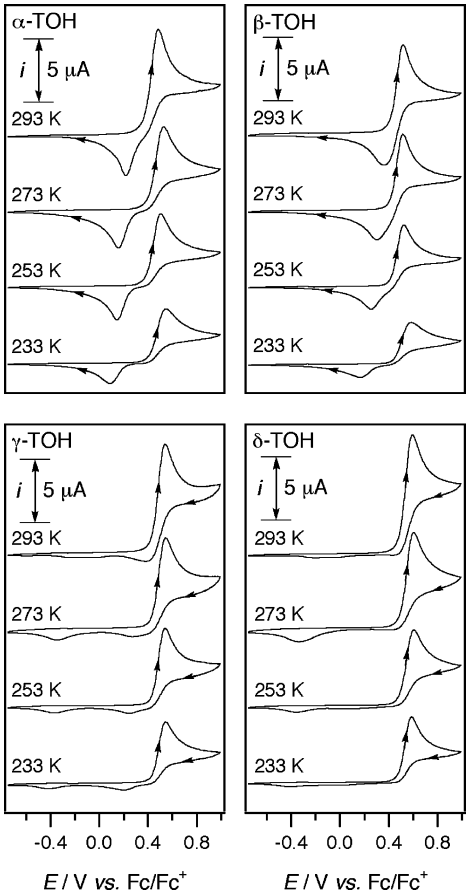

Figure 1. Cyclic voltammograms of 2 mM solutes recorded at a scan rate of 100 mV s^{-1} at a 1 mm diameter planar Pt electrode in CH_3CN with 0.25 M Bu_4NPF_6.

interactions of the solute with the electrode surface.[2,3]

$$\alpha\text{-TOH}^{+\bullet} \rightleftharpoons \alpha\text{-TO}^{\bullet} + H^{+} \quad (2)$$

Because the potentials of the voltammetric waves are influenced by the kinetics of the homogeneous reactions in Scheme 1, the peak potentials (or half-wave potentials) do not correspond to the thermodynamic formal potentials ($E°$). Therefore, it is difficult to calculate the exact electrode potentials for the different compounds, although the close similarities in the E_p^{ox} values in Figure 1 suggest that the formal potentials are very similar.

The voltammetric data obtained for β-TOH were the most alike to α-TOH, with clearly defined cathodic peaks (E_p^{red}) detected when the scan direction was reversed. Experiments previously performed on α-TOH indicated that the reverse peak was associated with the reduction of the phenoxonium ion back to the starting material; thus the close similarity in the voltammograms suggests that it is likely that β-TOH is also able to be reversibly oxidized to a phenoxonium ion. By analogy, the lack of a clearly defined reverse peak close to the main E_p^{ox} processes for γ- and δ-TOH at a scan rate of 0.1 V s^{-1} implies that their associated phenoxonium cations are relatively unstable (assuming they undergo the same mechanism as α-TOH).

Variable scan rate experiments in the range $\nu = 0.1-10$ V s^{-1} were performed on solutions of the tocopherols at 293 K. (Lower-temperature variable scan rate experiments are difficult because of the increased effects of solution resistance distorting the voltammograms.) For γ- and δ-TOH it was found that the peaks from −0.2 to −0.4 V evident when the scan direction was reversed (Figure 1) increased in magnitude as the scan rate was increased up to 1 V s^{-1}, then diminished as the scan rate was further increased up to 10 V s^{-1}. Concomitantly to the peaks from −0.2 to −0.4 V diminishing in magnitude at higher scan rates, new reduction peaks in the cyclic voltammograms of γ- and δ-TOH became evident at potentials ~0.3 V more negative than the main oxidation process, when the scan direction was reversed. Therefore, at the faster scan rates ($\nu = 10$ V s^{-1}), the voltammograms of γ- and δ-TOH began to appear similar to the voltammograms obtained for α- and β-TOH at slow scan rates ($\nu = 0.1$ V s^{-1}), with the reverse peaks detected in the cyclic voltammograms of γ- and δ-TOH at higher scan rates ($\nu = 10$ V s^{-1}) likely to be associated with the reduction of unstable phenoxonium cations. The observation that scan rates of at least 10 V s^{-1} were necessary to voltammetrically detect the phenoxonium cations (γ-TO^+ and δ-TO^+) indicates that their stabilities can be estimated at <1 s in CH_3CN at 293 K. Furthermore, the variable scan rate data indicate that the species responsible for the peaks from −0.2 to −0.4 V in the cyclic voltammograms of γ- and δ-TOH at slow scan rates are likely to be associated with a decomposition product of their associated phenoxonium ions. In contrast to γ- and δ-TOH, the voltammograms of α- and β-TOH did not change as the scan rate was varied in the range $\nu = 0.1-10$ V s^{-1}, except for the peak-to-peak separation increasing due to the effects of uncompensated solution resistance (Supporting Information).

The time scale of the CV experiments means that they can only indicate if oxidized (or reduced) species are stable for a few seconds or less, whereas bulk electrolysis experiments give an indication of stability over longer time intervals (normally greater than minutes). Electrolysis experiments on α-TOH in CH_3CN at 253 K indicated that the compound could be reversibly oxidized to α-TO^+ via a two-electron/one-proton process (Scheme 1, pathway 2), with the electrolysis reaction occurring over a period of a least 1 h.[2] Similar experiments performed on β-TOH also indicated the exhaustive transfer of almost two electrons per molecule ($n = 1.86$). However, the oxidized compound was not completely stable and partly decomposed during the course of the electrolysis reaction, resulting in the back-reduction reaction consuming only 0.78 electrons and indicating that ~60% of the β-TO^+ had decomposed/reacted (and indicating that β-TO^+ was significantly less stable than α-TO^+ over electrolysis time scales). Controlled potential electrolysis experiments performed on γ- and δ-TOH resulted in the transfer of more than two electrons per molecule (2.62 and 2.53, respectively), and the oxidized compounds quickly decomposed so that applying a reducing potential could not regenerate the starting materials (as expected based on the variable scan rate CV experiments described above). Absolute rate constants for the loss of the phenoxonium ions are difficult to calculate from electrolysis experiments because the cations are continually decomposing as they are being produced (at least for the β-, γ-, and δ-forms). However, it is clear that in CH_3CN the stability of the phenoxonium cations occurs in the order $\alpha \gg \beta \gg \gamma \approx \delta$, with CPE experiments indicating that α-TO^+ is stable for at least several hours (possibly much longer in extremely dry conditions)[2] and β-TO^+ stable for several minutes and variable scan rate CV experiments indicating γ-TO^+ and δ-TO^+ are stable for <1 s.

α-TO^+ has a characteristic UV−vis spectrum with absorbancies at ~22 000 and 33 500 cm^{-1} (in CH_3CN),[2] and it was expected that the other (β-, γ-, and δ-) tocopherol phenoxonium cations would have closely related spectra if they could be detected. In situ electrochemical/UV−vis spectroscopy per-

formed during the oxidation of β-TOH led to the detection of a spectrum very similar to that of α-TO^+ and with absorbancies at 22 400 and 34 400 cm^{-1}, which could also be assigned to β-TO^+. However, the spectrum showed additional bands at higher wavenumbers (37 500 and 39 000 cm^{-1}) that did not diminish when a reducing potential was applied and are associated with a reaction product of the phenoxonium cation (as expected based on the CPE experiments described above). The UV−vis spectra obtained during the oxidation of γ- and δ-TOH showed strong bands at 37 800 and 38 600 cm^{-1}, respectively, that were also associated with reaction products of their phenoxonium cations. (Their phenoxonium ions were too unstable to be detected in the OTTLE apparatus, even at low temperatures.) UV−vis spectra obtained during the oxidation of β-, γ-, and δ-TOH in CH_3CN are given in the Supporting Information.

3.2. Electrochemistry and UV−Vis Spectroscopy in CH_2Cl_2 Containing CF_3COOH. Cyclic voltammograms obtained in pure (neutral) CH_2Cl_2 were slightly different than those performed in CH_3CN due to the rate and equilibrium constants for the proton dissociation reaction in Scheme 1 (eq 2) changing in different solvents, thereby affecting the shapes of the voltammograms.[3] For α-TOH at 293 K, one anodic process was observed for the forward scan direction at approximately +0.55 V vs Fc/Fc^+ due to the oxidation of α-TOH and further oxidation of α-$TO^\bullet$ (overall a two-electron process; Scheme 1, pathway 2; Figure 2a). When the scan direction was reversed, two cathodic peaks (E_p^{red}) were detected at approximately +0.4 and +0.2 V vs Fc/Fc^+ that were associated with the reduction of α-$TOH^{+\bullet}$ and α-TO^+, respectively.[2,3] Therefore, at 293 K in CH_2Cl_2, the equilibrium constant in eq 2 is shifted toward the protonation reaction (compared to in CH_3CN), so that the cation radical can be voltammetrically detected. As the temperature was lowered, the equilibrium conditions for the proton dissociation reaction in eq 2 changed, resulting in the reverse (reductive) traces of the voltammograms altering in appearance. It appears that the equilibrium constant in eq 2 moves toward the deprotonation reaction as the temperature is lowered (hence the phenoxonium cation is the favored product), as the reverse sweep in the cyclic voltammogram at 233 K is dominated by the reduction of the phenoxonium ion (Figure 2a). The increasing cathodic current that is seen at less than −0.2 V in the cyclic voltammogram at 273 K (and to a lesser extent at 253 K) is a voltammetric-stripping peak associated with an adsorbed oxidized product.

It was believed that increasing the concentration of acid in solution would shift the equilibrium in eq 2 toward the cation radical and change the voltammograms from a two-electron process to a one-electron process at sufficiently high acid concentrations. Preliminary results on α-TOH in CH_3CN containing CF_3SO_3H were complicated by CH_3CN appearing to react with CF_3SO_3H at high acid concentrations.[2] CH_2Cl_2 containing CF_3COOH has been reported to be a more stable solvent mixture for generating and stabilizing cationic species,[14a] so it is the medium adopted for this study. Hexafluoro-2-propanol is also an excellent solvent for reducing the effects of adventitious reactive nucleophiles and stabilizing cation radicals, but it has a relatively high melting point (269 K) and so is not suitable for low-temperature experiments.[14b] Figure 2b shows the results that were obtained as CF_3COOH was added to solutions of α-TOH in CH_2Cl_2 at 233 K. As the acid concentration approached ~0.25 M, the separation between the E_p^{ox} and the E_p^{red} values (ΔE_{pp}) decreased, and the anodic (i_p^{ox}) and cathodic (i_p^{red}) peak currents became close to unity (although

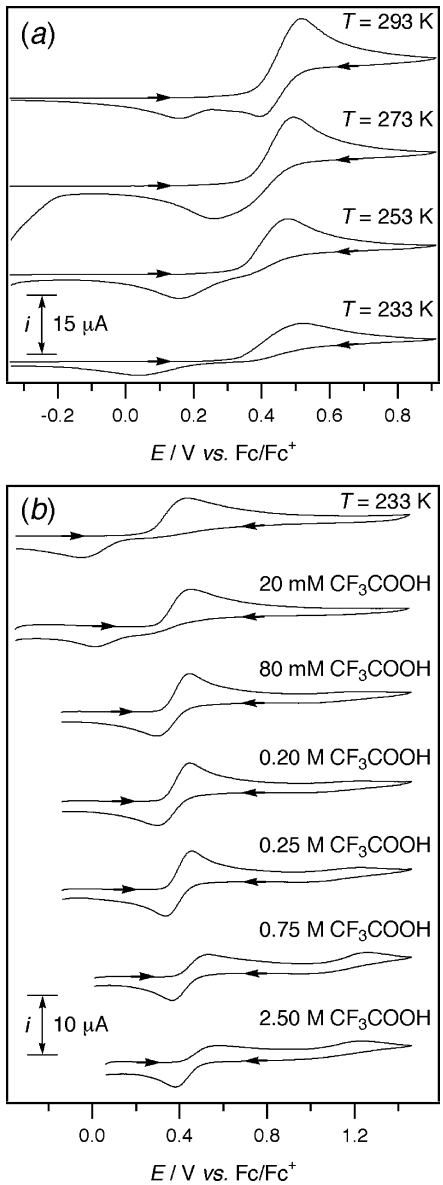

Figure 2. Cyclic voltammograms of 5 mM α-TOH recorded at a scan rate of 100 mV s^{-1} at a 1 mm diameter planar Pt electrode in CH_2Cl_2 with 0.25 M Bu_4NPF_6: (a) at varying temperature; (b) at varying concentration of CF_3COOH.

the respective peak currents remained almost constant). The overall process involved the chemically reversible transfer of two electrons (Scheme 1, pathway 2), with the increasing acid concentration shifting the equilibrium toward the intermediate cation radical and favoring the back-reaction (eq 2). At concentrations of acid >0.75 M, the i_p^{ox} and i_p^{red} values decreased to approximately half the values seen at lower acid concentrations. The decrease in peak currents was caused by a decrease in the number of electrons transferred due to the high acid concentration, completely inhibiting the proton dissociation reaction (eq 2) so that the oxidation process involved the transfer of one electron to form stable α-$TOH^{+\bullet}$. A new chemically reversible oxidation process also became evident at approximately +1.2 V (vs Fc/Fc^+) as the acid concentration increased, which was associated with the further one-electron oxidation of α-$TOH^{+\bullet}$ to form α-TOH^{2+} (Scheme 1, pathway 1).

At low acid concentrations (or with no acid) the oxidation of the dication is not evident because α-$TOH^{+\bullet}$ immediately dissociates to α-$TO^\bullet$, which is further oxidized to α-TO^+. The cyclic voltammograms in Figure 2b suggest that the dication is

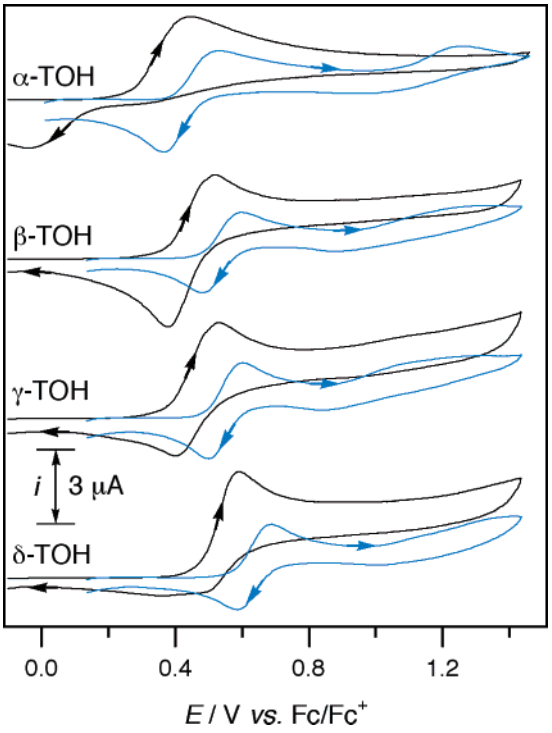

Figure 3. (Black lines) Cyclic voltammograms of 5 mM solutes recorded at a scan rate of 100 mV s^{-1} at a 1 mm diameter planar Pt electrode in CH_2Cl_2 with 0.25 M Bu_4NPF_6 at 253 K. (Blue lines) After the addition of 1 M CF_3COOH.

not particularly stable since only a small reverse peak is observed even at high acid concentrations. The apparent instability of the dication could be caused by it immediately losing a proton to form the phenoxonium cation or by it decomposing/reacting to form another compound. Analogous CV results were obtained for the α-TOH model compounds, (CH_3)α-TOH and (COOH)α-TOH, at variable temperatures and in the presence of acid (Supporting Information).

The voltammetric results obtained for *β*-, *γ*-, and *δ*-TOH in pure CH_2Cl_2 and CH_2Cl_2/CF_3COOH were similar to those for α-TOH. In pure CH_2Cl_2, cyclic voltammograms of *β*-, *γ*-, and *δ*-TOH showed a reverse reduction peak close to that of the forward oxidation process (E_p^{ox}) that was likely associated with the reduction of the cation radicals (Figure 3, black lines), due to the equilibrium in eq 2 shifting toward the protonation reaction. Furthermore, when 0.75 M CF_3COOH was added to the CH_2Cl_2 solutions, the peak currents for the oxidation processes decreased to approximately half that in the absence of acid, the E_p^{ox} values shifted to slightly higher potentials, and reverse reduction peaks (E_p^{red}) with i_p^{ox}/i_p^{red} ratios equal to unity were detected, suggesting the formation of stable cation radicals (Figure 3, blue lines). Another process was detected at more positive potentials (∼1.2−1.4 V vs Fc/Fc^+) in the presence of acid due to the further oxidation of the cation radicals (to possibly the dications). It was found that the acid itself provided a sufficiently strong oxidizing environment to spontaneously produce a few percent of the cation radicals, resulting in the solutions immediately turning pale yellow and allowing the detection of EPR spectra of paramagnetic species (Figure 4). Oxidizing the tocopherols under CPE conditions in CH_2Cl_2 containing 1.0 M CF_3COOH resulted in the EPR spectra in Figure 4 increasing in intensity due to an increase in concentration of the stable cation radicals.

In situ electrochemical/UV−vis measurements were conducted to determine the fate of $TOH^{+\bullet}$ and TOH^{2+} in acid

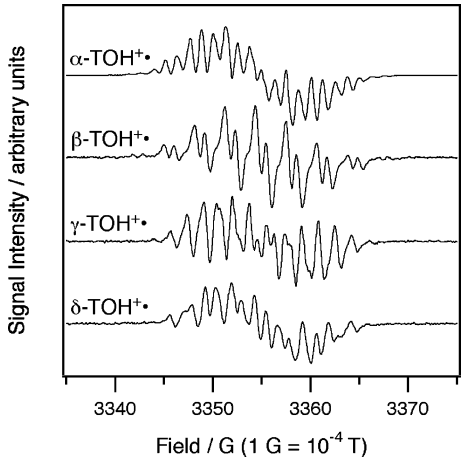

Figure 4. Continuous wave X-band EPR spectra of cation radicals formed by oxidizing 1 mM of the starting materials with 1 M CF_3COOH in CH_2Cl_2 at 293 K. The modulation amplitude is 0.2 G, the time constant is 100 ms, and the microwave frequency is 9.77 GHz.

conditions. The cyclic voltammetry experiments in Figure 2b indicated that ≥0.75 M CF_3COOH needed to be added to completely inhibit the deprotonation reaction in eq 2 and ensure that the electrochemical oxidation occurred by one electron to form $TOH^{+\bullet}$. Data from UV−vis experiments obtained during the oxidation of α-TOH in CH_2Cl_2 at 253 K are shown in Figures 5a and 5b, with the oxidation process occurring in two sequential steps. The spectrum of α-TOH should show only one band at ∼ 35 000 cm^{-1} (Figure 5a, dotted line).[2,4] The weaker bands that occur in the initial spectrum at 21 500, 22 600, and 32 500 cm^{-1} are due to the existence of several percent of $\alpha\text{-TOH}^{+\bullet}$ that forms immediately by chemical oxidation of α-TOH with the acid (as indicated from the EPR measurements above). When a positive potential was applied to the working electrode, the bands at 25 100, 22 600, and 32 500 cm^{-1} increased in intensity due to a buildup in concentration of the stable cation radical until maximum absorbancies were detected (Figure 5a, blue line).

After the cation radical had formed exhaustively from α-TOH, the spectra showed another change (under constant applied potential) where the bands at 21 500 and 22 600 cm^{-1} diminished in intensity (and a new low intensity broader band appeared at 21 800 cm^{-1}) and the band at 32 500 cm^{-1} shifted to 33 200 cm^{-1} and increased in intensity to form a final spectrum that was attributable to the phenoxonium cation (Figure 5b, red line).[2] The electronic transitions of $\alpha\text{-TOH}^{+\bullet}$ (blue lines) and $\alpha\text{-TO}^+$ (red line) appeared at surprisingly similar wavenumbers, although the intensity and peak shapes were sufficiently different to allow unambiguous characterization of each species (Figure 5). An isosbestic point appeared in the spectra during the transformation from $\alpha\text{-TOH}^{+\bullet}$ to $\alpha\text{-TO}^+$ at ∼42 000 cm^{-1} (Figure 5b) due to a decrease in intensity of the high-wavelength absorbancies. The UV−vis results are consistent with the one-electron oxidation of α-TOH to form $\alpha\text{-TOH}^{+\bullet}$ (Figure 5a) followed by the further one-electron oxidation of $\alpha\text{-TOH}^{+\bullet}$ to form $\alpha\text{-TOH}^{2+}$, which is not stable and quickly undergoes deprotonation to form $\alpha\text{-TO}^+$ (Figure 5b) (eq 3).

$$\alpha\text{-TOH}^{2+} \rightleftharpoons \alpha\text{-TO}^+ + H^+ \qquad (3)$$

An earlier study had suggested that the dication had substantial stability (for at least several hours) in CH_2Cl_2/CF_3COOH,[1] but our results (electrochemical and spectroscopic) indicate that the dication is too acidic to stabilize for longer than a few seconds. Repeating the UV−vis experiments with 50% acid (in

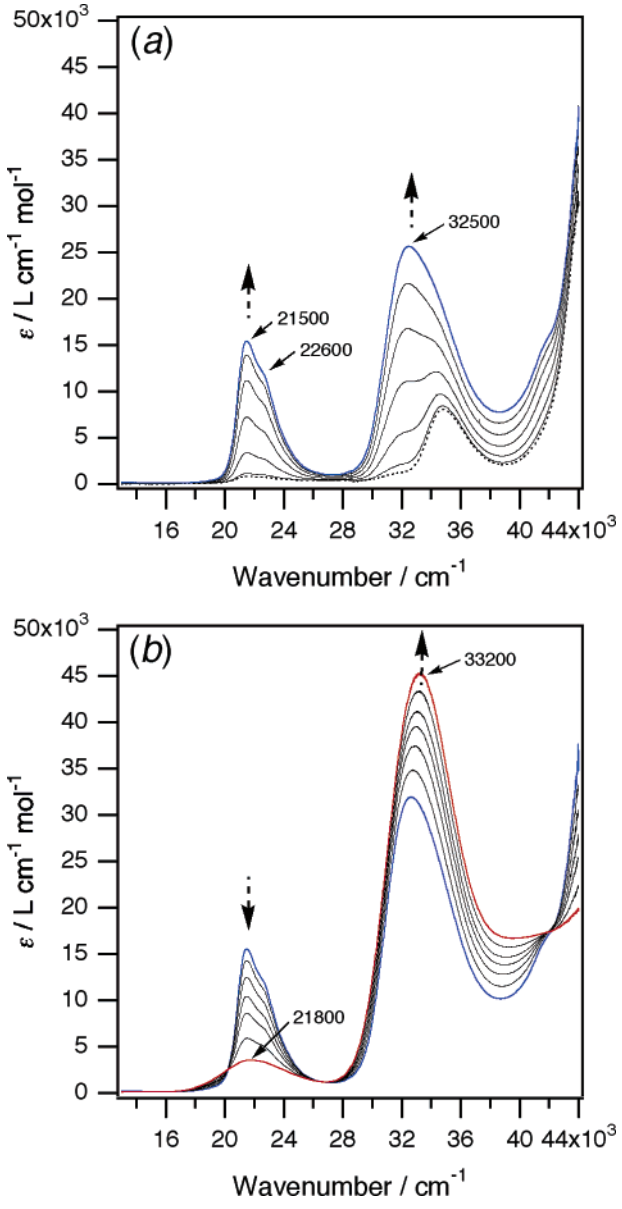

Figure 5. In situ UV−vis spectra obtained in CH_2Cl_2 containing 0.5 M Bu_4NPF_6 and 1 M CF_3COOH at 253 K during the sequential one-electron oxidation of 1 mM (a) α-TOH to α-$TOH^{+\bullet}$ and (b) α-$TOH^{+\bullet}$ to α-TO^+ (+ H^+). (Dotted line) α-TOH. (Black lines) Intermediate scans. (Blue lines) α-$TOH^{+\bullet}$. (Red line) α-TO^+.

CH_2Cl_2) did not prevent α-TO^+ from forming (from α-TOH^{2+}) immediately after α-$TOH^{+\bullet}$ had been exhaustively generated.

The spectral transformations in Figures 5a and 5b were reversible, so that applying a reducing potential at the end of the electrolysis resulted in exhaustively regenerating first α-$TOH^{+\bullet}$, then α-TOH in 100% yield. Because the dication is extremely acidic, it cannot survive for a sufficiently long time period under electrolysis conditions to enable its electrochemical reduction back to the monocation and then starting material. Therefore, the mechanism for the forward and reverse transformations in acidic conditions must be different. The forward oxidation reaction followed pathway 1 in Scheme 1 (with α-TOH^{2+} dissociating into α-TO^+), while the back-reduction mechanism followed pathway 2 in Scheme 1 (through α-$TO^\bullet$ undergoing immediate protonation to form α-$TOH^{+\bullet}$). When the oxidation reactions were conducted in pure CH_2Cl_2 (0.5 M Bu_4NPF_6), the UV−vis experiments indicated that the transformation went quickly to α-TO^+, with lesser amounts of α-$TOH^{+\bullet}$ being detected, due to α-$TOH^{+\bullet}$ dissociating into α-$TO^\bullet$, which was immediately oxidized to α-TO^+ (a similar result was observed in pure CH_3CN).[2] Therefore, it appears that on long electrolysis time scales all oxidation reactions in neutral, basic, and acidic dry media form α-TO^+ (Scheme 1), provided that the applied potential is sufficiently high. Similar electrochemical/UV−vis results were obtained for the α-TOH model compounds, (CH_3)α-TOH and (COOH)α-TOH, in the presence of acid (Supporting Information).

Electrochemical/UV−vis experiments performed at room temperature were identical to the lower-temperature experiments resulting in α-TOH being chemically reversibly oxidized first to α-$TOH^{+\bullet}$, then to α-TO^+. Previous UV−vis experiments performed in pure CH_3CN at 243 K indicated that α-TO^+ partially reacted with low levels of water (that are present at the millimolar level even in dry solvents) over long times (≤5% reaction over 4 h). Therefore, the high stability of α-TO^+ (and α-$TOH^{+\bullet}$) in CH_2Cl_2/CF_3COOH at ambient temperatures is likely to be due to the acid reacting preferentially with adventitious reactive nucleophiles (such as trace water), thereby protecting the cationic phenolic compounds from further reaction. A similar effect was observed for highly reactive $C_{60}^{+\bullet}$, which was able to be stabilized in a dry organic solvent containing a strong acid.[15] Electrochemical/UV−vis experiments performed during the oxidation of the water soluble analogue, (COOH)α-TOH, in H_2O containing 50% CF_3COOH showed no evidence of either the cation radical or the phenoxonium ion (Supporting Information). Instead a compound(s) was produced with strong absorbancies at ∼36 000−38 000 cm^{-1} (similar to the decomposition products of the other oxidized tocopherols in CH_3CN) that did not regenerate the starting material when a reducing potential was applied, indicating that the new absorbancies were due to different species than those given in Scheme 1. The instability of (COOH)α-$TOH^{+\bullet}$ in the presence of H_2O is not surprising, since phenolic cation radicals are known to be extremely acidic (eq 2) in aqueous systems;[16] therefore, (COOH)α-$TOH^{+\bullet}$ should rapidly deprotonate to form (COOH)α-$TO^\bullet$ that is immediately further oxidized to (COOH)α-TO^+. The K_{eq} value in eq 2 has been estimated to be $\sim 10^{-7}$ mol L^{-1} at 243 K in CH_3CN,[3] while in aqueous systems at ambient temperatures the K_a value (for (COOH)α-$TOH^{+\bullet}$) has been calculated to be much higher, with reports varying from 0.005[17] to 25 mol L^{-1}.[18] The instability of (COOH)α-TO^+ in H_2O must be due to an immediate hydrolysis reaction, even at low pH, since the experiments in CH_2Cl_2 indicate that the phenoxonium cation is stable in the presence of CF_3COO^-.

UV−vis spectra obtained during the oxidation of β-, γ-, and δ-TOH in CH_2Cl_2/CF_3COOH were partially the same as those obtained during the oxidation of α-TOH. The initial one-electron oxidation produced stable cation radicals with characteristic bands at ∼ 22 000−23 000 and 32 500 cm^{-1} (Figure 6, blue lines) that could be reduced back to the starting materials, indicating that the cation radicals were very stable. The further one-electron oxidation of β-$TOH^{+\bullet}$ appeared to produce a compound with a similar UV−vis spectrum to α-TO^+, suggesting that β-TO^+ was also forming. However, the UV−vis spectrum of β-TO^+ was complicated by the presence of additional peaks, and the spectrum of the starting material could only be partially regenerated when a reducing potential was applied, indicating that β-TO^+ was not completely stable in CH_2Cl_2 containing CF_3COOH. The UV−vis data obtained during the oxidation of γ-$TOH^{+\bullet}$ and δ-$TOH^{+\bullet}$ provided no evidence for the presence of γ-TO^+ or δ-TO^+ and instead indicated that the phenoxonium ions were very unstable even in the presence

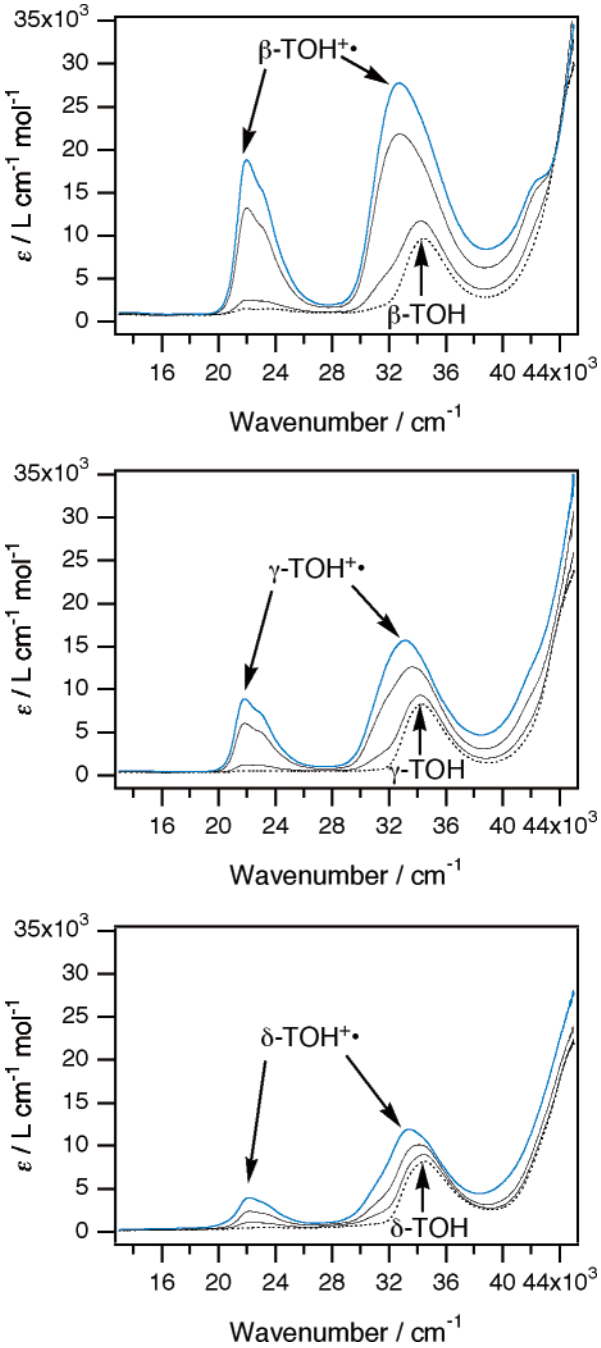

Figure 6. In situ UV−vis spectra obtained in CH_2Cl_2 containing 0.5 M Bu_4NPF_6 and 1 M CF_3COOH at 253 K during the one-electron oxidation of 1 mM solute. (Dotted lines) Starting material. (Black lines) Intermediate scans. (Blue lines) Cation radicals.

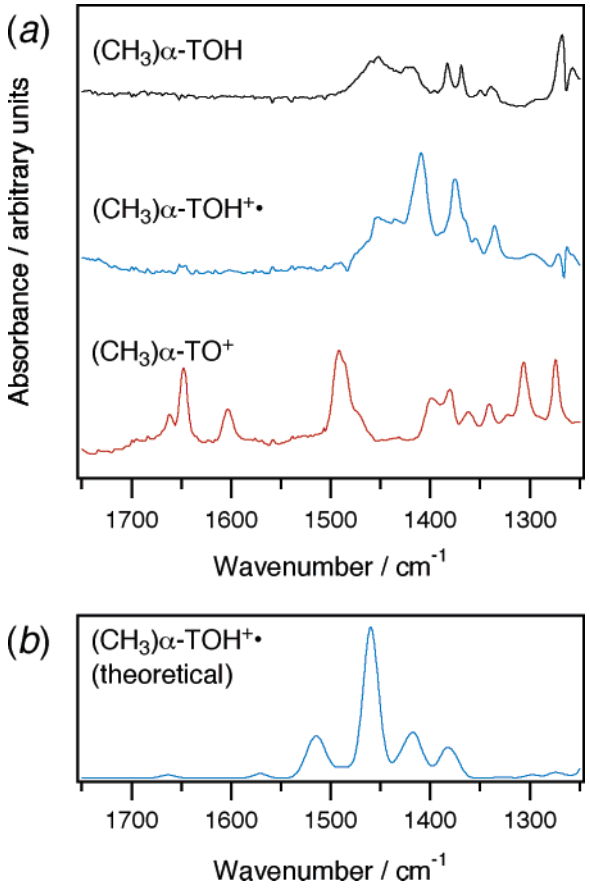

Figure 7. (a) In situ ATR-FTIR spectra obtained in CH_2Cl_2 containing 0.5 M Bu_4NPF_6 and 1 M CF_3COOH at 253 K during the sequential one-electron oxidation of 1 mM (a) α-TOH to α-$TOH^{+\bullet}$ and (b) α-$TOH^{+\bullet}$ to α-TO^+ (+ H^+). (b) Theoretical (unshifted) infrared spectrum of α-$TOH^{+\bullet}$.

of acid. The observation that β-TO^+, γ-TO^+, and δ-TO^+ were unstable in the presence of acid (as well as in neutral conditions) suggests that the phenoxonium cations are themselves inherently unstable rather than the instability occurring through a higher reactivity of the intermediate phenoxyl radicals. Since the oxidation in acid occurs via pathway 1 in Scheme 1, the intermediate phenoxyl radicals are bypassed on the way to the formation of the phenoxonium cations.

3.3. Infrared Spectroscopy in CH_2Cl_2 Containing CF_3COOH. Infrared spectra were obtained by in situ electrochemically oxidizing the phenolic starting material in a controlled potential electrolysis cell that contained an ATR-FTIR sensor.[2,9] The IR experiments were more difficult to perform than the UV−vis experiments because of relatively low sensitivity of the ATR-FTIR device combined with strong interference in the infrared from the solvent, electrolyte, and acid. Even though a background spectrum could be obtained, the electrolysis procedure necessitates that ions must move between the working and the auxiliary compartments of the electrolysis cell as the reaction progresses to maintain charge neutrality. Thus, as the oxidation occurred, PF_6^- and CF_3COO^- transferred from the auxiliary into the working electrode compartment, while concomitantly Bu_4N^+ transferred from the working into the auxiliary electrode compartment. It was found that a background "free" area existed in the range of ~1350−1750 cm^{-1}, which fortuitously is a region where characteristic transitions are observed for phenolic/quinoid compounds.

Due to the close similarity in the UV−vis spectra between the different cation radicals and model compounds, it was believed that the infrared spectrum of the highly soluble model compound, (CH3)α-TOH, would give a representative spectrum of a phenolic cation radical upon oxidation in CH_2Cl_2/CF_3-COOH. We are not aware of infrared spectra of any other phenolic cation radicals for comparison purposes, although the resonance Raman spectrum over a similar wavenumber range has been reported for transitory (COOH)α-$TOH^{+\bullet}$ generated in aqueous acid conditions.[18]

The IR spectra obtained during the oxidation of 0.05 M (CH3)α-TOH in CH_2Cl_2 containing 0.5 M Bu_4NPF_6 and 1 M CF_3COOH are shown in Figure 7a. The one-electron oxidation of (CH3)α-TOH (measured by coulometry) produced the spectrum that could be assigned to (CH3)α-$TOH^{+\bullet}$. The spectrum is quite similar to the starting material with no bands

evident in the 1750−1500 cm^{-1} region. The further one-electron oxidation of $(CH_3)\alpha$-$TOH^{+\bullet}$ produced the spectrum that could be assigned to $(CH_3)\alpha$-TO^+,[2,3] confirming the results of the UV−vis experiments that indicated that the dication quickly deprotonates to form the phenoxonium ion. The spectrum of the starting material could be regenerated by applying a sufficiently negative potential (and the transfer of two electrons).

The calculated theoretical infrared spectrum for the cation radical is given in Figure 7b, which predicts no strong bands in the 1750−1500 cm^{-1} region. The calculated spectrum appears to be shifted to higher wavenumbers by ca. 50 cm^{-1}, which is similar to the level of accuracy found for the theoretical spectra of the starting material and phenoxonium ion.[3] The four strong bands in the theoretical spectrum appear to correlate with the four intense bands observed in the experimental spectrum between 1300 and 1500 cm^{-1}. The weak bands in the calculated spectrum at 1660 and 1570 cm^{-1} theoretically correspond to symmetric and asymmetric aromatic ring stretches, respectively, and are not evident in the experimental spectrum, although very weak bands would not be detectable with the present ATR sensor. A resonance Raman study in aqueous acid solution detected a single strong band in the 1300−1800 cm^{-1} region at 1620 cm^{-1}, which was assigned to a C═C ring stretching mode of $(COOH)\alpha$-$TOH^{+\bullet}$.[18] The symmetric and asymmetric aromatic ring stretches and the carbonyl stretching mode are much stronger in the infrared spectrum of the phenoxonium ion and occur in the experimental spectrum at 1605, 1650, and 1670 cm^{-1}.[3] The calculations predict that the C−OH and C−O stretching modes for $(CH_3)\alpha$-$TOH^{+\bullet}$ occur at 1470 and 1460 cm^{-1}, respectively, which likely correlate with the strong band observed in the experimental spectrum at ∼1410 cm^{-1}.

4. Discussion

The spectroscopic and electrochemical results in this study have indicated that all of the tocopherols undergo the electrochemical mechanism in Scheme 1, with the most important difference relating to the stabilities of the phenoxonium ions. α-TOH appears to be unusual for two reasons. First, its phenoxonium cation is stable in neutral conditions, which is in contrast to most phenoxonium cations that are extremely unstable species under any conditions.[19] The instabilities of β-TO^+, γ-TO^+, and δ-TO^+ are not simply due to increased reactivity with water (since α-TO^+ is fully stable in CH_2Cl_2/CF_3COOH) and must instead relate to specific properties introduced by the degree of methyl substitution. Second, the transformation between α-TOH and α-TO^+ in neutral organic solvents is completely chemically reversible on both the seconds and the hours time scales. Complete chemical reversibility in an ECE mechanism is unusual and occurs in this case because the back-reaction in eq 2 is very fast (essentially diffusion-controlled)[3] and because the equilibrium constant for eq 2 favors the back-reaction (consequently α-$TOH^{+\bullet}$ is relatively nonacidic in organic solvents).[2,3] There are a number of intriguing factors relating to the high stability of α-TO^+ (compared to the other tocopherols) that suggest its existence may be more important than simple coincidence.

The principal mode of action of vitamin E in mammalian tissues is thought to relate to its ability to act as an antioxidant, essentially preventing living cell membranes (lipids) from turning rancid and decomposing,[20,21] and most of the chemical studies on vitamin E have focused on its ability to act as a radical scavenger. In theory, α-TO^+ could have oxidant properties (if it were to exist in vivo) since it should be easily reduced by the semiquinone radical of ubiquinone (which is partly responsible for in vivo superoxide formation) or reduced by superoxide itself to form either α-TO^- or α-TOH (depending on the availability of protons).[2]

SCHEME 2: Potential Coenzymatic Mode of Action of α-TOH[a]

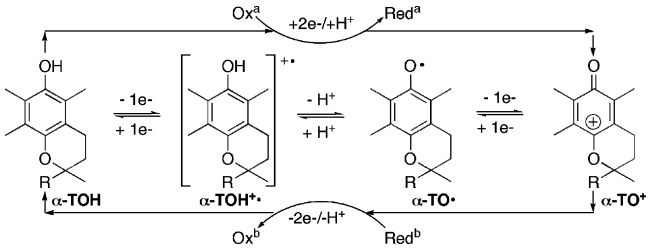

[a] Ox^a/Red^a and Ox^b/Red^b are different oxidizing and reducing agents. The redox reactions occur in two sequential one-electron steps, while the redox agents responsible for each individual step are not necessarily the same.

While vitamin E is certainly capable of acting as a sacrificial compound to limit cell membrane deterioration, there is a growing body of evidence that it has other biological functions that involve specific interactions with other components of the cell, such as proteins and enzymes.[22] The uptake of vitamin E in mammalian systems is a highly selective process with several binding proteins having been identified.[22,23] The most important protein (or at least the most well-known) is the α-tocopherol transfer protein (α-TTP), which is responsible for delivering tocopherols to very low density lipoproteins (VLDLs), which are then transferred and delivered to peripheral cells.[22] α-TTP is found in a number of vital organs including the liver, brain, retina, and uterus and at a low level in fibroblasts and lymphocytes.[24] The binding affinity of α-TTP for the α-, β-, γ-, and δ-forms of the tocopherols occurs in the order $\alpha > \beta > \gamma \gg \delta$,[25] which is similar to the relative stability of the phenoxonium ions found in this work. Non-antioxidant functions of α-TOH were first proposed in the early 1990s when it was discovered that α-TOH displayed much different biological effects than the less methylated forms,[26] even though they shared similar antioxidant capacities (established in model micelle systems).[27] Thus it was speculated that the selective uptake of α-TOH was because it has a specific non-antioxidant function over the other tocopherols.

Protein kinases are a family of enzymes that regulate critical biological processes such as memory, hormone responses, and cell growth. Inhibition of protein kinase C (PKC) activity was found to be the basis of vascular smooth muscle cell growth arrest induced by α-TOH.[22,26] β-TOH is ineffective at inhibition of PKC but prevents the inhibitory effect of α-TOH, whereas γ- and δ-TOH have no effect on PKC.[22] The inhibition of PKC by α-TOH has been supported by a number of studies on different cell types including fibroblasts, macrophages, mesangial cells, monocytes, and neutrophils.[28] Therefore, there must exist an important mechanistic feature associated with α-TOH (compared to the β-, γ-, and δ-forms) that causes it to react/interact in a special way with PKC, which is currently missing from the biological literature. The reversible nature of the transformations in Scheme 1 and the unusual high stability of α-TO^+ allow the opportunity for α-TOH (and possibly β-TOH, but not γ- or δ-TOH) to take part in an enzymatic electron/proton exchange reaction such as given in Scheme 2. A similar (two-electron but two-proton) process occurs in the coenzyme ubiquinone 10, which is thought to function as a mobile redox proton carrier in the energy transducing membranes of mitochondria and chloroplasts.[29] The reaction in Scheme 2 can occur under approximately pH neutral conditions and at low potentials

(~0.1−0.5 V vs Fc/Fc^+), well within the oxidizing/reducing conditions accessible in biological systems.

In conclusion, the recent biological studies on vitamin E indicate that α-TOH has unique function(s) compared to those of the other tocopherols, which cannot be explained by their proposed antioxidant properties. This study has demonstrated that there are significant differences in the electrochemical behaviors of the tocopherols, with only α-TOH forming a highly stable phenoxonium cation following electrochemical oxidation. To date, the stability of the phenoxonium ions and cation radicals of all the tocopherols have been measured under optimal conditions in neutral or acidic CH_3CN or CH_2Cl_2. The electrochemical and spectroscopic data obtained in this, and earlier,[1−3] studies provide a useful database with which to test for the existence and stability of the cationic compounds of α-TOH in more biologically relevant matrixes.

Acknowledgment. G.J.W. thanks the Research School of Chemistry for the award of a Summer Scholarship, and R.D.W. thanks the Australian Research Council for the award of a QEII Research Fellowship.

Supporting Information Available: Additional CV and in situ electrochemical UV−vis data for α-, β-, γ-, and δ-TOH, (CH_3)α-TOH, and (COOH)α-TOH under a range of conditions, UV−vis spectra of α-TOH, α-$TOH^{+\bullet}$, and α-TO^+ plotted in nanometers (taken from the data in Figure 5), and a summary of results from theoretical calculations on α-$TOH^{+\bullet}$ (Cartesian coordinates, number of imaginary frequencies, and total energies). This material is available free of charge via the Internet at http://pubs.acs.org.

References and Notes

(1) Svanholm, U.; Bechgaard, K.; Parker, V. D. *J. Am. Chem. Soc.* **1974**, *96*, 2409−2413.

(2) Williams, L. L.; Webster, R. D. *J. Am. Chem. Soc.* **2004**, *126*, 12441−12450 and references therein.

(3) Lee, S. B.; Lin, C. Y.; Gill, P. M. W.; Webster, R. D. *J. Org. Chem.* **2005**, *70*, 10466−10473.

(4) Nanni, E. J., Jr.; Stallings, M. D.; Sawyer, D. T. *J. Am. Chem. Soc.* **1980**, *102*, 4481−4485.

(5) Webster, R. D. *Electrochem. Commun.* **1999**, *1*, 581−584.

(6) Smith, L. I.; Ungnade, H. E.; Hoehn, H. H.; Wawzonek, S. *J. Org. Chem.* **1939**, *4*, 311−317.

(7) Fry, A. J.; Britton, W. E. In *Laboratory Techniques in Electroanalytical Chemistry*; Kissinger, P. T., Heineman, W. R., Eds.; Marcel Dekker: New York, 1984; Chapter 13.

(8) (a) Webster, R. D.; Heath, G. A.; Bond, A. M. *J. Chem. Soc., Dalton Trans.* **2001**, 3189−3195. (b) Arnold, D. P.; Hartnell, R. D.; Heath, G. A.; Newby, L.; Webster, R. D. *J. Chem. Soc., Chem. Commun.* **2002**, 754−755.

(9) (a) Webster, R. D. *J. Chem. Soc., Perkin Trans. 2* **2002**, 1882−1888. (b) Webster, R. D. *Electrochem. Commun.* **2003**, *5*, 6−11.

(10) Kong, J.; White, C. A.; Krylov, A. I.; Sherrill, C. D.; Adamson, R. D.; Furlani, T. R.; Lee, M. S.; Lee, A. M.; Gwaltney, S. R.; Adams, T. R.; Ochsenfeld, C.; Gilbert, A. T. B.; Kedziora, G. S.; Rassolov, V. A.; Maurice, D. R.; Nair, N.; Shao, Y.; Besley, N. A.; Maslen, P. E.; Dombroski, J. P.; Daschel, H.; Zhang, W.; Korambath, P. P.; Baker, J.; Byrd, E. F. C.; Van Voorhis, T.; Oumi, M.; Hirata, S.; Hsu, C.-P.; Ishikawa, N.; Florian, J.; Warshel, A.; Johnson, B. G.; Gill, P. M. W.; Head-Gordon, M.; Pople, J. A. *J. Comput. Chem.* **2000**, *21*, 1532−1548.

(11) *Spartan '04 for Macintosh*; Wavefunction Inc.: Irvine, CA.

(12) Lin, C. Y.; George, M. W.; Gill, P. M. W. *Aust. J. Chem.* **2004**, *57*, 365−370.

(13) Gill, P. M. W.; Johnson, B. G.; Pople, J. A. *Chem. Phys. Lett.* **1993**, *209*, 506−512.

(14) (a) Hammerich, O.; Parker, V. D. *Acta Chem. Scand. B* **1982**, *36*, 63−64. (b) Eberson, L.; Hartshorn, M. P.; Persson, O.; Radner, F. *Chem. Commun.* **1996**, 2105−2112.

(15) Webster, R. D.; Heath, G. A. *Phys. Chem. Chem. Phys.* **2001**, *3*, 2588−2594.

(16) Hammerich, O.; Svensmark, B. In *Organic Electrochemistry*, 3rd ed.; Lund, H., Baizer, M. M., Eds.; Marcel Dekker: New York, 1991; Chapter 16.

(17) Thomas, M. J.; Bielski, B. H. J. *J. Am. Chem. Soc.* **1989**, *111*, 3315−3319.

(18) Parker, A. W.; Bisby, R. H. *J. Chem. Soc., Faraday Trans.* **1993**, *89*, 2873−2878.

(19) (a) Speiser, B.; Rieker, A. *J. Chem. Res., Synop.* **1977**, 314−315. (b) Vigalok, A.; Rybtchinski, B.; Gozin, Y.; Koblenz, T. S.; Ben-David, Y.; Rozenberg, H.; Milstein, D. *J. Am. Chem. Soc.* **2003**, *125*, 15692−15693.

(20) (a) Burton, G. W.; Ingold, K. U. *Acc. Chem. Res.* **1986**, *19*, 194−201. (b) Bowry, V. W.; Ingold, K. U. *J. Org. Chem.* **1995**, *60*, 5456−5467. (c) Bowry, V. W.; Ingold, K. U. *Acc. Chem. Res.* **1999**, *32*, 27−34.

(21) (a) Packer, L.; Witt, E. H.; Tritschler, H. J. *Free Radical Biol. Med.* **1995**, *19*, 227−250. (b) Traber, M. G.; Arai, H. *Annu. Rev. Nutr.* **1999**, *19*, 343−355. (c) Finkel, T.; Holbrook, N. J. *Nature* **2000**, *408*, 239−247. (d) Wang, X.; Quinn, P. J. *Prog. Lipid Res.* **1999**, *38*, 309−336. (e) Wang, X.; Quinn, P. J. *Mol. Membr. Biol.* **2000**, *17*, 143−156. (f) Niki, E.; Noguchi, N. *Acc. Chem. Res.* **2004**, *37*, 45−51.

(22) (a) Azzi, A.; Stocker, A. *Prog. Lipid Res.* **2000**, *39*, 231−255. (b) Ricciarelli, R.; Zingg, J.-M.; Azzi, A. *J. Biol. Chem.* **2002**, *383*, 457−465. (c) Azzi, A.; Ricciarelli, R.; Zingg J.-M. *FEBS Lett.* **2002**, *519*, 8−10.

(23) (a) Dutta-Roy, A. K.; Leishman, D. J.; Gordon, M. J.; Campbell, F. M.; Duthie, G. G. *Biochem. Biophys. Res. Commun.* **1993**, *196*, 1108−1112. (b) Kostner, G. M.; Oettl, K.; Jauhiainen, M.; Ehnholm, C.; Esterbauer, H.; Dieplinger, H. *Biochem. J.* **1995**, *305*, 659−667. (c) Zimmer, S.; Stocker, A.; Sarbolouki, M. N.; Spycher, S. E.; Sassoon, J.; Azzi, A. *J. Biol. Chem.* **2000**, *275*, 25672−25680.

(24) (a) Copp, R. P.; Wisniewski, T.; Hentati, F.; Larnaout, A.; Ben Hamida, M.; Kayden, H. J. *Brain Res.* **1999**, *822*, 80−87. (b) Yokota, T.; Shiojiri, T.; Gotoda, T.; Arita, M.; Arai, H.; Ohga, T.; Kanda, T.; Suzuki, J.; Imai, T.; Matsumoto, H.; Harino, S.; Kiyosawa, M.; Mizusawa, H.; Inoue, K. *Ann. Neurol.* **1997**, *41*, 826−832. (c) Jishage, K.; Arita, M.; Igarashi, K.; Iwata, T.; Watanabe, M.; Ogawa, M.; Ueda, O.; Kamada, N.; Inoue, K.; Arai, H.; Suzuki, H. *J. Biol. Chem.* **2001**, *276*, 1669−1672. (d) Tamaru, Y.; Hirano, M.; Kusaka, H.; Ito, H.; Imai, T.; Ueno, S. *Neurology* **1997**, *49*, 584−588.

(25) Hosomi, A.; Arita, M.; Sato, Y.; Kiyose, C.; Ueda, T.; Igarashi, O.; Arai, H.; Inoue, K. *FEBS Lett.* **1997**, *409*, 105−108.

(26) (a) Boscoboinik, D.; Szewczyk, A.; Hensey, C.; Azzi, A. *J. Biol. Chem.* **1991**, *266*, 6188−6194. (b) Tasinato, A.; Boscoboinik, D.; Bartoli, G. M.; Maroni, P. Azzi, A. *Proc. Natl. Acad. Sci. U.S.A.* **1995**, *92*, 12190−12194.

(27) Pryor, W. A.; Cornicelli, J. A.; Devall, L. J.; Tait, B.; Trivedi, B. K.; Witiak, D. T.; Wu, M. *J. Org. Chem.* **1993**, *58*, 3521−3532.

(28) (a) Devaraj, S.; Li, D.; Jialal, I. *J. Clin. Invest.* **1996**, *98*, 756−763. (b) Freedman, J. E.; Farhat, J. H.; Loscalzo, J.; Keaney, J. F., Jr. *Circulation* **1996**, *94*, 2434−2440. (c) Tada, H.; Ishii, H.; Isogai, S. *Metabolism* **1997**, *46*, 779−784.

(29) Mitchell, P. In *Advances in Membrane Biochemistry and Bioenergetics*; Kim, C. H., Tedeschi, H., Diwan, J. J., Salerno, J., Eds.; Plenum Press: New York, 1988; pp 25−52.